C-terminally truncated, kidney-specific variants of the WNK4 kinase lack several sites that regulate its activity

Murillo-de-Ozores, Adrián Rafael ; Rodríguez-Gama, Alejandro ; Bazúa-Valenti, Silvana ; Leyva-Ríos, Karla ; Vázquez, Norma ; Pacheco-Álvarez, Diana ; De La Rosa-Velázquez, Inti A ; Wengi, Agnieszka ; Stone, Kathryn L ; Zhang, Junhui ; Loffing, Johannes ; Lifton, Richard P ; Yang, Chao-Ling ; Ellison, David H ; Gamba, Gerardo ; Castañeda-Bueno, Maria

Abstract: WNK lysine-deficient protein kinase 4 (WNK4) is an important regulator of renal salt handling. Mutations in its gene cause pseudohypoaldosteronism type II, mainly arising from overactivation of the renal Na+/Cl- cotransporter (NCC). In addition to full-length WNK4, we have observed faster migrating bands (between 95 and 130 kDa) in Western blots of kidney lysates. Therefore, we hypothesized that these could correspond to uncharacterized WNK4 variants. Here, using several WNK4 antibodies and WNK4-/- mice as controls, we showed that these bands indeed correspond to short WNK4 variants that are not observed in other tissue lysates. LC-MS/MS confirmed these bands as WNK4 variants that lack C-terminal segments. In HEK293 cells, truncation of WNK4's C terminus at several positions increased its kinase activity toward Ste20-related proline/alanine-rich kinase (SPAK), unless the truncated segment included the SPAK-binding site. Of note, this gain-of-function effect was due to the loss of a protein phosphatase 1 (PP1)-binding site in WNK4. Cotransfection with PP1 resulted in WNK4 dephosphorylation, an activity that was abrogated in the PP1-binding site WNK4 mutant. The electrophoretic mobility of the in vivo short variants of renal WNK4 suggested that they lack the SPAK-binding site and thus may not behave as constitutively active kinases toward SPAK. Finally, we show that at least one of the WNK4 short variants may be produced by proteolysis involving a Zn2+-dependent metalloprotease, as recombinant full-length WNK4 was cleaved when incubated with kidney lysate.

DOI: https://doi.org/10.1074/jbc.RA118.003037

C-terminally truncated, kidney-specific variants of the WNK4 kinase lack several sites that regulate its activity

Received for publication, March 20, 2018, and in revised form, June 14, 2018 Published, Papers in Press, June 19, 2018, DOI 10.1074/jbc.RA118.003037

Adrián Rafael Murillo-de-Ozores,[a1] Alejandro Rodríguez-Gama,[b] Silvana Bazúa-Valenti,[b] Karla Leyva-Ríos,[c] Norma Vázquez,[b] Diana Pacheco-Álvarez,[c] Inti A. De La Rosa-Velázquez,[d] Agnieszka Wengi,[e] Kathryn L. Stone,[f] Junhui Zhang,[g] Johannes Loffing,[e] Richard P. Lifton,[g,h] Chao-Ling Yang,[i,j] David H. Ellison,[i,j] Gerardo Gamba,[b,k,l] and Maria Castañeda-Bueno[k2]

From the [a]Facultad de Medicina, and [b]Instituto de Investigaciones Biomédicas, Universidad Nacional Autónoma de México, Mexico City 14080, Mexico, the [c]Escuela de Medicina, Universidad Panamericana, Mexico City 03920, Mexico, the [d]Genomics Laboratory, RAI, Universidad Nacional Autónoma de México-Instituto Nacional de Ciencias Médicas y Nutrición Salvador Zubirán, Mexico City 14080, Mexico, the [e]Institute of Anatomy and Swiss National Centre of Competence in Research "Kidney Control of Homeostasis," University of Zurich, Zurich 8057, Switzerland, the [f]MS and Proteomics Resource, W. M. Keck Biotechnology Resource Laboratory and [g]Department of Genetics, Yale University School of Medicine, New Haven 06510, Connecticut, the [h]Laboratory of Human Genetics and Genomics, Rockefeller University, New York, New York 10065, the [i]Division of Nephrology and Hypertension, Department of Medicine, Oregon Health and Science University, Portland, Oregon 97239, the [j]Veterans Affairs Portland Health Care System, Portland, Oregon 97239, the [k]Department of Nephrology and Mineral Metabolism, Instituto Nacional de Ciencias Médicas y Nutrición Salvador Zubirán, Mexico City 14080, Mexico, and the [l]Tecnológico de Monterrey, Escuela de Medicina y Ciencias de la Salud, Monterrey 64710, Nuevo León, Mexico

Edited by Roger J. Colbran

WNK lysine-deficient protein kinase 4 (WNK4) is an important regulator of renal salt handling. Mutations in its gene cause pseudohypoaldosteronism type II, mainly arising from overactivation of the renal Na^+/Cl^- cotransporter (NCC). In addition to full-length WNK4, we have observed faster migrating bands (between 95 and 130 kDa) in Western blots of kidney lysates. Therefore, we hypothesized that these could correspond to uncharacterized WNK4 variants. Here, using several WNK4 antibodies and $WNK4^{-/-}$ mice as controls, we showed that these bands indeed correspond to short WNK4 variants that are not observed in other tissue lysates. LC-MS/MS confirmed these bands as WNK4 variants that lack C-terminal segments. In HEK293 cells, truncation of WNK4's C terminus at several positions increased its kinase activity toward Ste20-related proline/alanine-rich kinase (SPAK), unless the truncated segment included the SPAK-binding site. Of note, this gain-of-function effect was due to the loss of a protein phosphatase 1 (PP1)-binding site in WNK4. Cotransfection with PP1 resulted in WNK4 dephosphorylation, an activity that was abrogated in the PP1-binding site WNK4 mutant. The electrophoretic mobility of the *in vivo* short variants of renal WNK4 suggested that they lack the SPAK-binding site and thus may not behave as constitutively active kinases toward SPAK. Finally, we show that at least one of the WNK4 short variants may be produced by proteolysis involving a Zn^{2+}-dependent metalloprotease, as recombinant full-length WNK4 was cleaved when incubated with kidney lysate.

WNK lysine-deficient protein kinase 4 (WNK4)[3] is a serine-threonine kinase that is present in several tissues, including brain, lungs, liver, and heart, with the highest expression levels observed in kidney, colon, and testes (1). Mutations occurring within a specific motif in WNK4, the acidic motif, produce the human genetic disease pseudohypoaldosteronism type II (PHAII) (2). This disease features hypertension, hyperkalemia, metabolic acidosis, and marked sensitivity to thiazide diuretics, alterations that are thought to be mainly due to higher basal activity of the renal thiazide–sensitive Na^+/Cl^- cotransporter (NCC), which is specifically expressed in the distal convoluted tubule (DCT) of the nephron (3, 4). Decreased activity levels of the K^+ channel ROMK and Na^+ channel ENaC may also contribute (5). The acidic motif of WNK4 constitutes the binding site for the cullin-RING E3 ubiquitin ligase complex formed by cullin 3, Kelch-like 3, and an E3 ring ubiquitin ligase, which regulates the degradation of the kinase (6, 7). Thus, PHAII mutations occurring in this motif decrease the degradation rate of the kinase, leading to its overexpression.

WNK4-knockout mice present markedly decreased levels of NCC expression and virtually no NCC phosphorylation. Accordingly, the phenotype of WNK4-knockout mice resembles that of patients with Gitelman disease, featuring hypoten-

This work was supported by National Institutes of Health Grant DK51496 (to G. G., C.-L. Y., and D. H. E.) and Conacyt Grants 23 (to G. G.) and 257726 (to M. C.-B.). The authors declare that they have no conflicts of interest with the contents of this article. The content is solely the responsibility of the authors and does not necessarily represent the official views of the National Institutes of Health.

This article contains Tables S1–S3 and Figs. S1–S4.

[1] Graduate student from the "Programa de Doctorado en Ciencias Biomédicas, Universidad Nacional Autónoma de México (UNAM)" and recipient of CONACYT Fellowship 606808.

[2] To whom correspondence should be addressed. Tel.: 5255-5487-0900 (ext. 2511); E-mail: mcasta85@yahoo.com.mx.

[3] The abbreviations used are: WNK4, WNK lysine-deficient protein kinase 4; ROMK, renal outer medullary potassium channel; ENaC, epithelial Na channel; PHAII, pseudohypoaldosteronism type II; NCC, Na^+/Cl^- cotransporter; DCT, distal convoluted tubule; SPAK, Ste20-related proline/alanine-rich kinase; pSPAK, SPAK phosphorylation; RACE, rapid amplification of cDNA ends; HRP, horseradish peroxidase; COPAS, Complex Object Parametric Analyzer and Sorter.

sion, hypokalemia, and metabolic alkalosis, which is caused by inactivating mutations in NCC (8). Thus, WNK4 is a key regulator of NCC, and its activity is essential to maintain basal NCC activity levels.

WNK4 promotes NCC activation through the phosphorylation of the T-loop of the Ste20-related proline/alanine–rich kinase (SPAK), which in turn phosphorylates key residues for NCC activation located in the N-terminal, cytoplasmic domain of the cotransporter (9, 10). In contrast, the regulatory effect of WNK4 on ROMK and ENaC appears to be independent of kinase activity (11, 12). Recently, it was shown that knock-in mice carrying a constitutively active form of SPAK in the DCT develop PHAII (3). Thus, WNK4's direct effects on ROMK and ENaC do not seem to be essential to develop the disease.

WNK4 kinase activity is regulated by at least two different mechanisms. Binding of a chloride ion within a site located near the active site of the kinase stabilizes an inactive conformation and prevents kinase activity (13, 14). Thus, at high intracellular chloride concentrations ($[Cl^-]_i$), chloride ions remain bound to these sites, inhibiting WNK4 activity. Conversely, when $[Cl^-]_i$ decreases, dissociation of Cl^- ions allows kinase activation. This mechanism has been shown to be important for NCC modulation in response to changes in extracellular K^+ concentration ($[K^+]_e$), because changes in $[K^+]_e$ affect the intracellular Cl^- concentration of DCT cells (15).

The second known regulatory mechanism of WNK4 kinase activity involves phosphorylation of at least two sites, Ser-64 and Ser-1196, located within the regulatory N- and C-terminal domains of WNK4, respectively (16). Phosphorylation of these sites promotes kinase activation; it can be conducted by protein kinase C or protein kinase A, and it is stimulated, for example, in response to AT1 receptor activation by angiotensin II. So far, the mechanism linking phosphorylation to kinase activation is unknown; however, both the N-terminal and C-terminal domains of WNK4 have long been thought to play a regulatory role (17–19), and several functional motifs have been described in the C-terminal domain (16). For instance, the acidic domain (2), two PF2-like domains (20), two putative PP1-binding motifs (21), one RF*X*V motif (22), and the HQ motif important for WNK dimerization (23, 24) have been described within the C-terminal domain of WNK4.

During our recent characterization of the WNK4-knockout mouse strain (8), we noticed that several bands smaller than that corresponding to the full-length WNK4 were observed in blots of renal tissues performed with an antibody directed against an N-terminal epitope; these were absent in samples from the knockout animals, ruling them out as nonspecific signals. Thus, we hypothesized that these bands could correspond to previously unrecognized variants of WNK4. Here, we present evidence that confirms the identity of these short bands as WNK4 short variants that lack a portion of the C-terminal domain. In addition, the characterization of these short variants of WNK4 has led us to the identification of a *bona fide* PP1-binding site located at the final portion of WNK4's C terminus, which regulates WNK4 phosphorylation levels and, thus, kinase activity.

Results

WNK4 short variants lacking a segment of the C-terminal domain are observed in mouse kidney lysates

Mouse kidney lysates from $WNK4^{+/+}$ and $WNK4^{-/-}$ mice were analyzed by Western blotting using antibodies directed against three distinct WNK4 epitopes. Using two different antibodies directed against N-terminal epitopes, we observed, in addition to the band corresponding to the full-length protein, at least two smaller bands that were absent in the $WNK4^{-/-}$ mouse samples (Fig. 1*A* and Fig. S1*A*). These smaller bands were more abundant in samples from $TgWNK4^{PHAII}$ mice (4) (Fig. S1*B*) and were not detected when an antibody directed against a C-terminal WNK4 epitope was used (Fig. 1*B*). These results suggest that the small bands observed correspond to shorter variants of WNK4, with an intact N-terminal domain and probably lacking a segment of the C terminus. These shorter WNK4 variants appear to be kidney-specific, as they were not observed in lysates from testis, brain, and lung when analyzed with a WNK4 N-terminal antibody (Fig. 1*C*).

Full-length WNK4 and the shorter variants were immunoprecipitated from mouse kidney lysates and separated by SDS-PAGE (Fig. 1*D*). Bands were excised from gel and individually analyzed by MS (LC-MS/MS). For the excised gel sample containing the full-length protein, tryptic peptides generated from the whole length of the protein were detected, including peptides from the C-terminal region (Fig. 1*E* and Table S1). In contrast, for the gel sample containing the smaller WNK4 variants, only peptides generated from the N-terminal and middle region of the protein were observed, whereas no peptides from the last portion of the C-terminal domain were detected (Fig. 1*E* and Table S2). This confirms the identity of the small-sized bands observed in Western blots as smaller variants of WNK4 lacking a portion of the C terminus. In addition, given that the 781–787 peptide was observed in the sample corresponding to the short WNK4 variants (Table S2), at least the segment comprising amino acid residues 1–787 must be present in the longest of the short variants. It should be noted that the large tryptic peptide comprising residues 788–970 was not expected to be detected in these assays due to its large size, and thus, the absence of detection of this peptide may not have been due to absence of this segment in the short WNK4 variants.

C-terminally truncated WNK4 constructs are more active than full-length WNK4, as long as they contain the C-terminal SPAK-binding site

To understand the impact that C-terminal truncations may have on WNK4 activity, we generated several WNK4 mutant constructs in which STOP codons were inserted at strategic positions between functional motifs (Fig. 2*A*). This allowed us to test the impact of the additive elimination of these motifs. The activity of these constructs was tested in HEK293 cells that were cotransfected with SPAK. SPAK phosphorylation (pSPAK; Ser-373) was measured as an indicator of WNK4 activity. Almost all mutant constructs presented a higher level of activity than WNK4-WT (Fig. 2, *B* and *C*), which was comparable with the activity of the WNK4-L319F mutant that is considered to be a constitutively active mutant due to

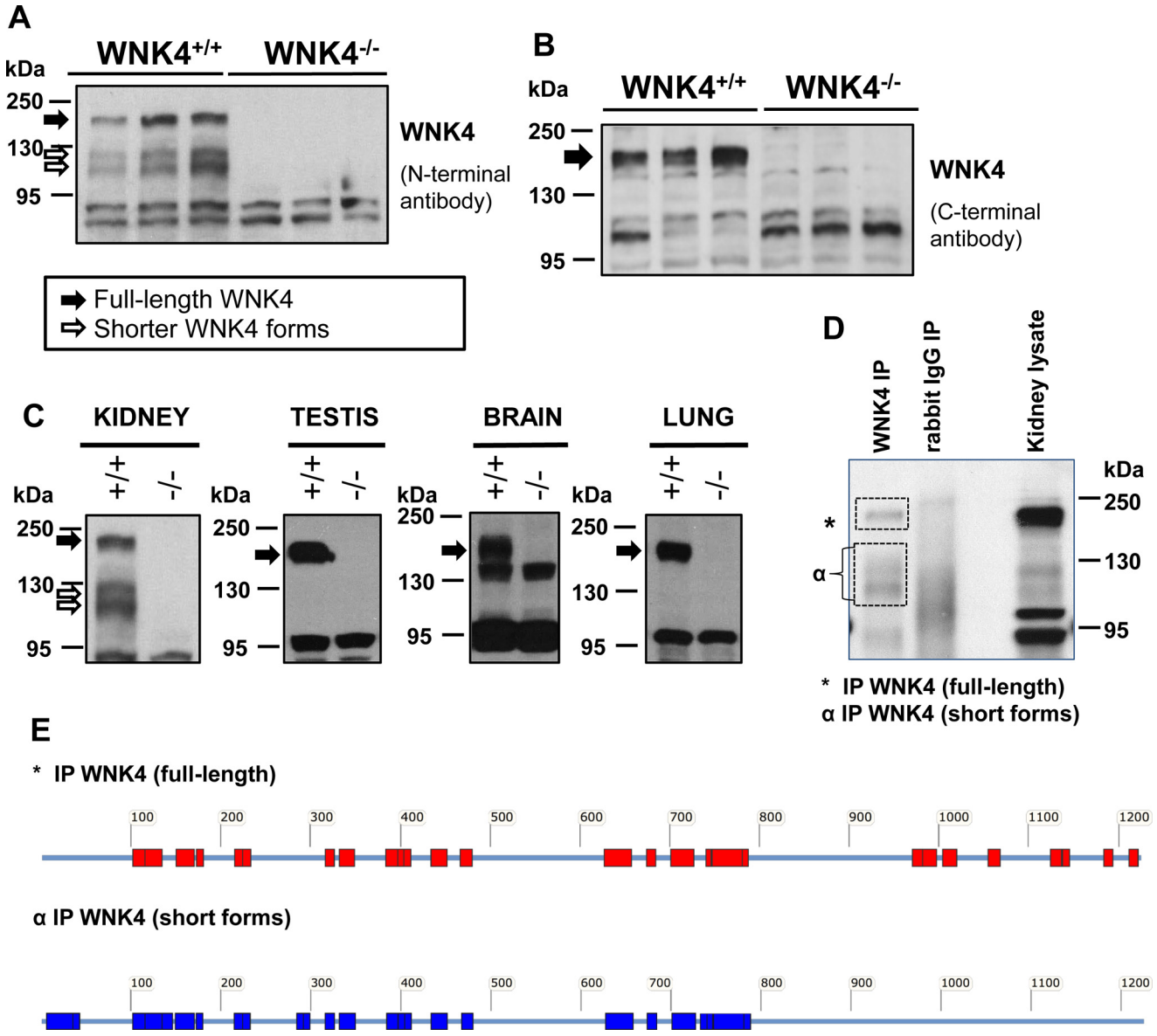

Figure 1. Identification of WNK4 short variants present in kidney lysates. *A*, Western blotting of kidney lysates of WNK4$^{+/+}$ and WNK4$^{-/-}$ mice using an antibody that recognizes an N-terminal epitope of WNK4 (residues 2–167 of mouse WNK4) (WNK4 antibody A described under "Experimental procedures") (41). In addition to the band corresponding to the full-length WNK4 (indicated by a *black arrow*), this antibody detects at least two additional bands that are absent in the WNK4$^{-/-}$ samples (*white arrows*). This image has been previously used by Yang *et al.* (41), as part of the WNK4 antibody characterization; however, no emphasis was made at this time in the WNK4 short variants. *B*, same as in *A*, but an antibody that recognizes a C-terminal epitope of WNK4 was used (residues 1221–1243 of human WNK4) (antibody B) (8). Only the full-length WNK4 is observed. Thus, the smaller bands observed in *A* might correspond to shorter WNK4 variants lacking a segment of the C-terminal region. *C*, Western blots performed with samples of different tissues from WNK4$^{+/+}$ and WNK4$^{-/-}$ mice using the same antibody as in *A*. The additional bands corresponding to putative WNK4 short variants are only observed in kidney lysates. Different exposure times are presented for clarity: 30 s for kidney and testis, 10 min for brain and lung. *D*, WNK4 was immunoprecipitated from kidney lysates and subjected to SDS-PAGE. A gel fragment containing the full-length band and another one containing the smaller bands were excised as indicated, and the extracted tryptic peptides were analyzed by LC-MS/MS. *E*, schematic representation of the peptides observed in LC-MS/MS assays. For the full-length band, peptides from every domain of WNK4 were observed. For the short bands, WNK4 peptides were observed, but none of them corresponded to the C-terminal region (see also Tables S1 and S2). This confirms that the smaller bands correspond to short WNK4 fragments that lack a portion of the C-terminal region. *IP*, immunoprecipitation.

impaired chloride binding in the kinase domain (14). This effect depended on WNK4 catalytic activity, because it was prevented by introduction of the D318A mutation, which renders the kinase catalytically inactive (Fig. 2*F* and Fig. S2*A*) (25). The only mutant construct that did not present higher activity levels than WNK4-WT was WNK4-R996X. Because this mutant is only 35 amino acid residues shorter than the WNK4-T1029X mutant, and the only functional motif known in this segment is the SPAK-binding site comprising residues 996–999 (RF*X*V motif) (26), we deduced that the lower pSPAK levels observed with this mutant were due to the loss of this motif. We also assessed T-loop phosphorylation of the truncated mutants WNK4-K1211X and -T1029X as an alternative indicator of activation level. For both mutants, we observed higher T-loop phosphorylation levels than for WNK4-WT (Fig. 2, *D* and *E*). Finally, a representative WNK4-truncated mutant was tested for its ability to promote NCC activation in *Xenopus laevis* oocytes. In accordance with the results obtained in HEK293 cells, the

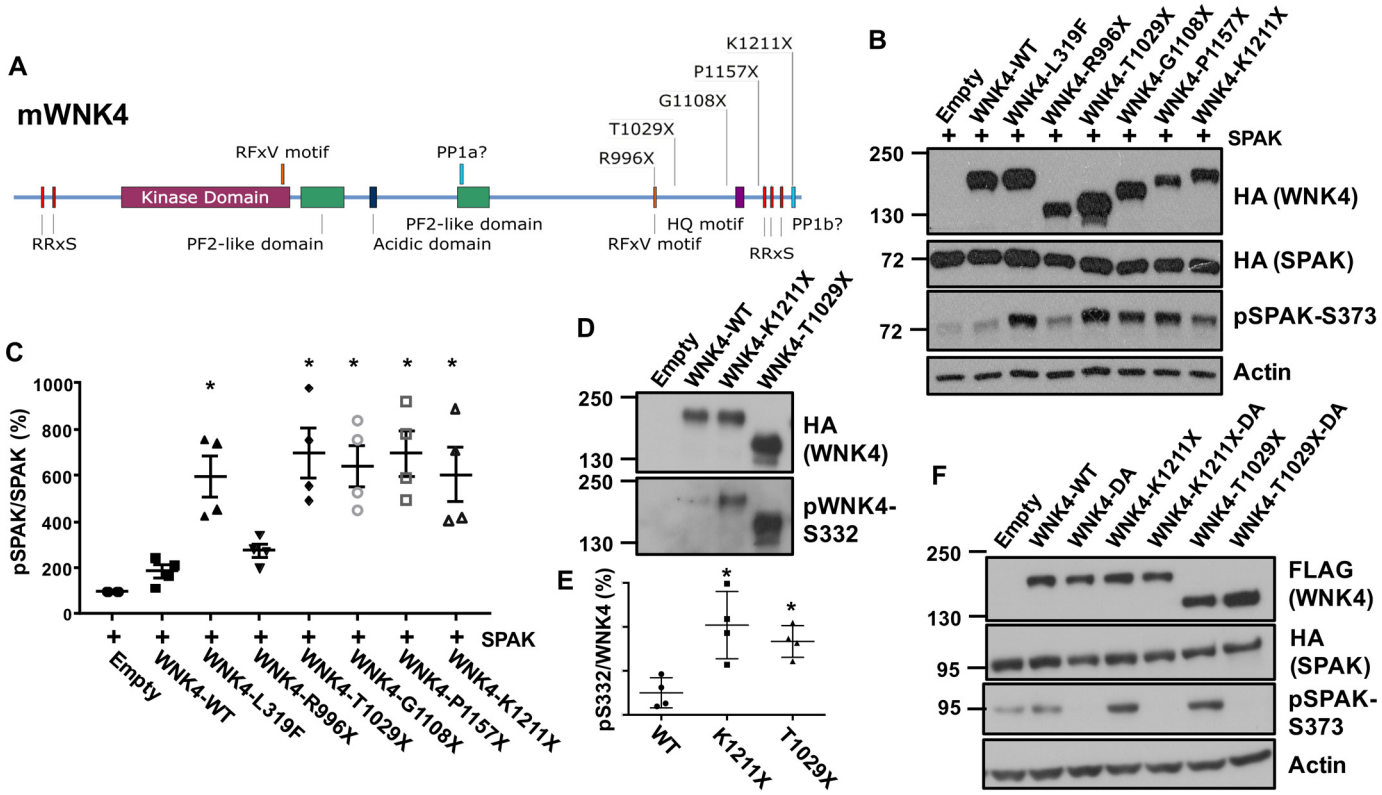

Figure 2. Effect of C-terminal deletions on WNK4 kinase activity. *A, schematic representation* of WNK4 protein depicting its important domains and motifs. The position of insertion of STOP codons for the generation of the truncated mutants is indicated. *RRxS*, sites of phosphorylation by protein kinase C/protein kinase A (16); *RFXV*, motifs presenting consensus sequence for SPAK interaction (22); *PF2-like*, domain similar to the PF2 domain present in SPAK/OSR1 that in SPAK/OSR1 forms the binding pocket for the RF*X*V motif present in WNKs and Slc12 cotransporters (20, 47); *Acidic domain*, motif that mediates interaction with the KLHL3–CUL3–RING complex (6) (PHAII-causing mutations found in WNK4 lie within this motif); *PP1a/PP1b*, putative protein phosphatase 1–binding sites (21); *HQ motif*, motif implicated in WNK homo- and heterodimerization (23). *B*, representative Western blots of lysates from HEK293 cells transfected with SPAK-HA and different WNK4 mutants to assess their effect on SPAK phosphorylation. *C*, densitometric analysis of blots presented in *A* shows that C-terminally truncated WNK4 constructs have increased activity compared with full-length WNK4, and similar to that of the chloride-insensitive, constitutively active mutant (L319F), unless the SPAK-binding site is absent. Data are mean ± S.E. (*error bars*); *, $p < 0.05$ *versus* WNK4-WT, $n \geq 4$ in at least three independent experiments. *D*, HEK293 cells were transfected with WNK4-WT or the indicated truncated mutants. WNK4 was immunoprecipitated, and T-loop phosphorylation (Ser-332) was assessed by Western blotting. *E*, densitometric analysis shows that the baseline T-loop phosphorylation of the truncated mutants WNK4-K1211X and -T1029X is higher than that of WNK4-WT. *, $p < 0.05$ *versus* WNK4-WT, $n = 4$ in at least three independent experiments. *F*, HEK293 cells were transfected with WNK4 truncated mutants that were made catalytically inactive by introduction of the D318A mutation. These mutants were unable to phosphorylate SPAK, showing that the higher pSPAK levels observed in the presence of catalytically active truncated mutants are due to higher WNK4 kinase activity.

WNK4-T1029X mutant promoted NCC activation, whereas no NCC activation was observed with the WNK4-WT under the experimental conditions tested (Fig. S2*B*).

Elimination of a PP1-binding site located at the final portion of the C-terminal domain increased activity of the truncated WNK4 mutants

We noted that the only common feature between the four truncated mutants that presented higher activity levels than WNK4-WT was the absence of the last 12 amino acid residues of the protein. Within this region, a motif presenting the consensus sequence for interaction with PP1 is present (K*X*V*X*F) (27). Lin *et al.* (21) have shown that when this site and a second putative PP1-binding site (located at positions 695–699) are mutated, the WNK4–PP1 interaction is lost. In our hands, however, the WNK4–PP1 interaction was preserved in a WNK4 mutant lacking both putative PP1-binding sites (here termed PP1a and PP1b) (Fig. 3*A*). However, when only a fragment of WNK4's C terminus was expressed (residues 770–1222), which contains only the PP1b site, the absence of this site disrupted the interaction with PP1. This result suggests that the PP1b site is indeed a PP1-binding site but that, in addition to the PP1a and PP1b sites, additional motifs present in WNK4 may be involved in the interaction.

We hypothesized that the gain of function observed in the truncated WNK4 mutants was due to the loss of the PP1b site. We thus tested whether elimination of the PP1a, PP1b, or both sites could replicate the gain of function observed with the truncated mutants. Interestingly, we observed that only the individual elimination of the PP1b site replicated the gain-of-function effect (Fig. 3, *B* and *C*) and that when the PP1a site was mutated in addition to the PP1b site, the gain-of-function effect was lost.

We next tested the effect of the cotransfection of the different PP1 isoforms (PP1α, PP1β, and PP1γ) on the phosphorylation levels of WNK4-WT at previously described phosphorylation sites (RR*X*S sites) (16). We observed that coexpression of PP1α and PP1γ promoted WNK4 dephosphorylation, whereas coexpression of PP1β had no effect (Fig. 3*D*). The inability of PP1β to dephosphorylate WNK4 may be because it binds to

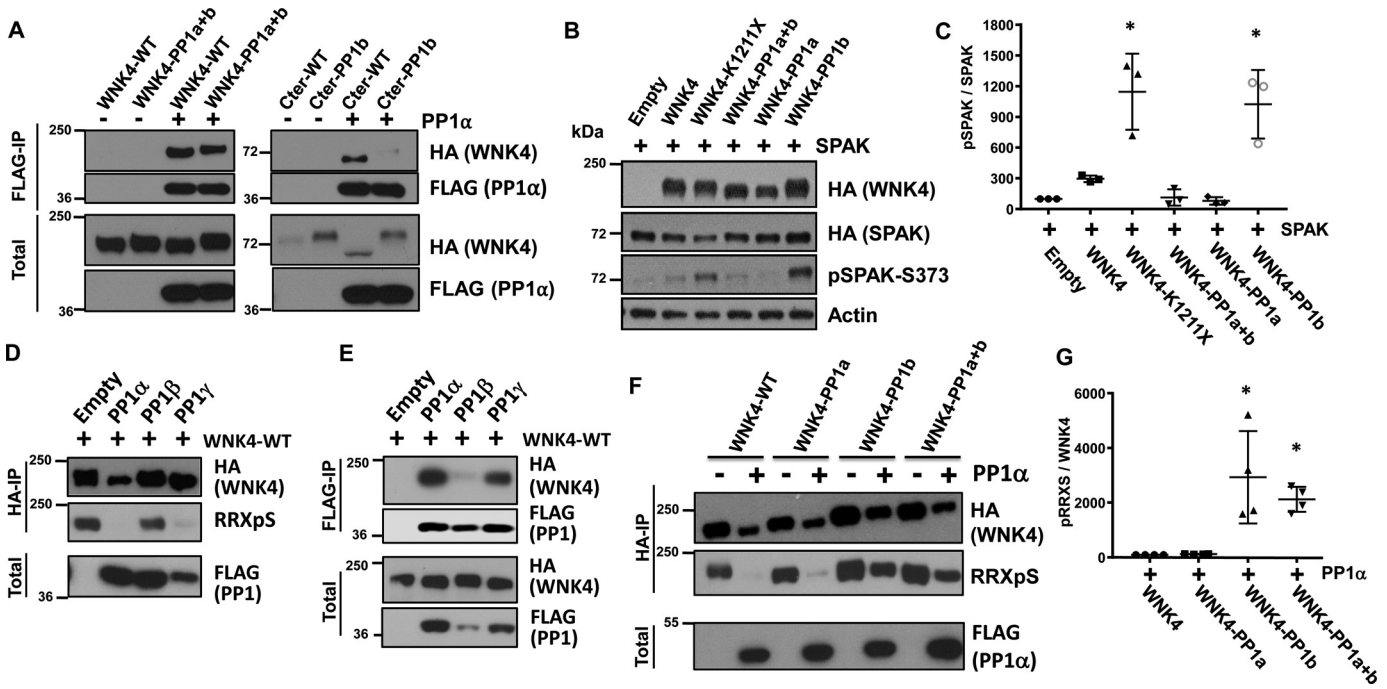

Figure 3. A PP1-binding site located in the C terminus of WNK4 regulates its phosphorylation and activity. *A*, co-immunoprecipitation assay of WNK4 and PP1α. HEK293 cells were transfected with PP1α and either full-length WNK4 (*left*) or a C-terminal fragment of WNK4 (residues 770–1222) (*right*). The effect of elimination of the predicted PP1-binding sites was assessed. A shift in the electrophoretic mobility of the WNK4–PP1a+b mutant is observed (migrates slower). This is even more evident with the C-terminal fragment harboring the PP1b mutation. Such a shift may be related to the phosphorylation levels of the protein, given that, as shown in the following panels, elimination of the PP1b site prevents WNK4 dephosphorylation. *B*, Western blots of lysates from HEK293 cells transfected with WNK4 constructs in which the putative PP1-binding sites were mutated (21). Their effect on pSPAK was assessed. PP1a mutant contains mutations V697A/T698A/F699A, and PP1b contains V1213A/T1214A/F1215A. PP1b mutant is more active than WT. *C*, results of quantitation of blots represented in *B*. Data are mean ± S.E. (*error bars*). *, $p < 0.05$ *versus* WNK4-WT, $n = 3$. *D*, HEK293 cells were cotransfected with WNK4-WT and different PP1 isoforms. Before Western blots were performed, WNK4 was immunoprecipitated from cell lysates to eliminate signal detected from other proteins with the RRXpS antibody. Only PP1α and PP1γ promoted WNK4 dephosphorylation at RR*X*S sites. *E*, WNK4 interaction with the different PP1 isoforms was assessed by co-immunoprecipitation. Similar results were observed in three independent experiments. *F*, cells were cotransfected with PP1α and the indicated WNK4 mutants. WNK4 was immunoprecipitated, and blots were performed with the indicated antibodies. PP1α promotes dephosphorylation of WNK4 at RR*X*S sites (41) unless the PP1b site is mutated. *G*, results of quantitation of blots presented in *F*: phosphorylation levels of WNK4 in the presence of PP1α. Data are mean ± S.E.; *, $p < 0.05$ *versus* WNK4-WT, $n = 4$. *IP*, immunoprecipitation.

WNK4 with lower affinity than the other isoforms (Fig. 3*E*). The effect of PP1α co-expression on WNK4 phosphorylation levels depended on PP1 catalytic activity (Fig. S3).

Finally, we tested the effect of PP1α cotransfection on the phosphorylation levels of the PP1 binding mutants. We observed that the presence of the PP1b mutation (either alone or together with the PP1a mutation) prevented the PP1α-mediated dephosphorylation of WNK4 (Fig. 3, *F* and *G*), whereas the WNK4–PP1a mutant behaved similarly to the WT.

Altogether, these results suggest that PP1α and PP1γ are important regulators of WNK4 phosphorylation levels and that they require the presence of the C-terminal binding site, here described as PP1b, to achieve dephosphorylation. Impaired dephosphorylation of WNK4 in the presence of the PP1b mutation leads to kinase activation. This activation is lost in the presence of the PP1a mutation despite high WNK4 phosphorylation levels observed in this double mutant, suggesting that the PP1a mutation impairs the kinase activity of WNK4. Of note, the PP1a site lies within a region of WNK4 that has been described to have a PF2-like fold similar to the one present in SPAK and OSR1. This PF2-like domain present in SPAK and OSR1 has been implicated in the binding of RF*X*V motifs present in WNK kinases and SLC12 cotransporters (26), and thus, it may play a role in a key functional WNK4 interaction.

At least one of the short WNK4 variants observed in kidney lysates may be the product of a proteolytic event

The presence of two different kidney-specific short variants of the SPAK kinase has been described. McCormick *et al.* (28) reported the existence of an alternative transcript of SPAK that was identified through a 5′-RACE assay. Markadieu *et al.* (29) showed that a proteolytic activity present in kidney lysates produces a cleavage in SPAK that generates SPAK fragments truncated at the N terminus similar to those observed in kidney lysates. Interestingly, it was recently shown that kidney lysates of mice that express SPAK only in the DCT, from a transgene carrying SPAK's ORF, display the same pattern of bands in SPAK blots compared with those observed with lysates of WT mice. This suggests that the shorter variants of SPAK are primarily produced by proteolytic cleavage and are present in the DCT (3).

To investigate the origin of the short variants of WNK4 observed in kidney samples, we performed 3′-RACE assays designed to detect alternative transcripts that would produce WNK4 proteins lacking a portion of the C terminus (Table S3) (30). Only the previously described full-length transcript of WNK4 was successfully amplified by this method. In addition, we searched for alternative WNK4 transcripts in published

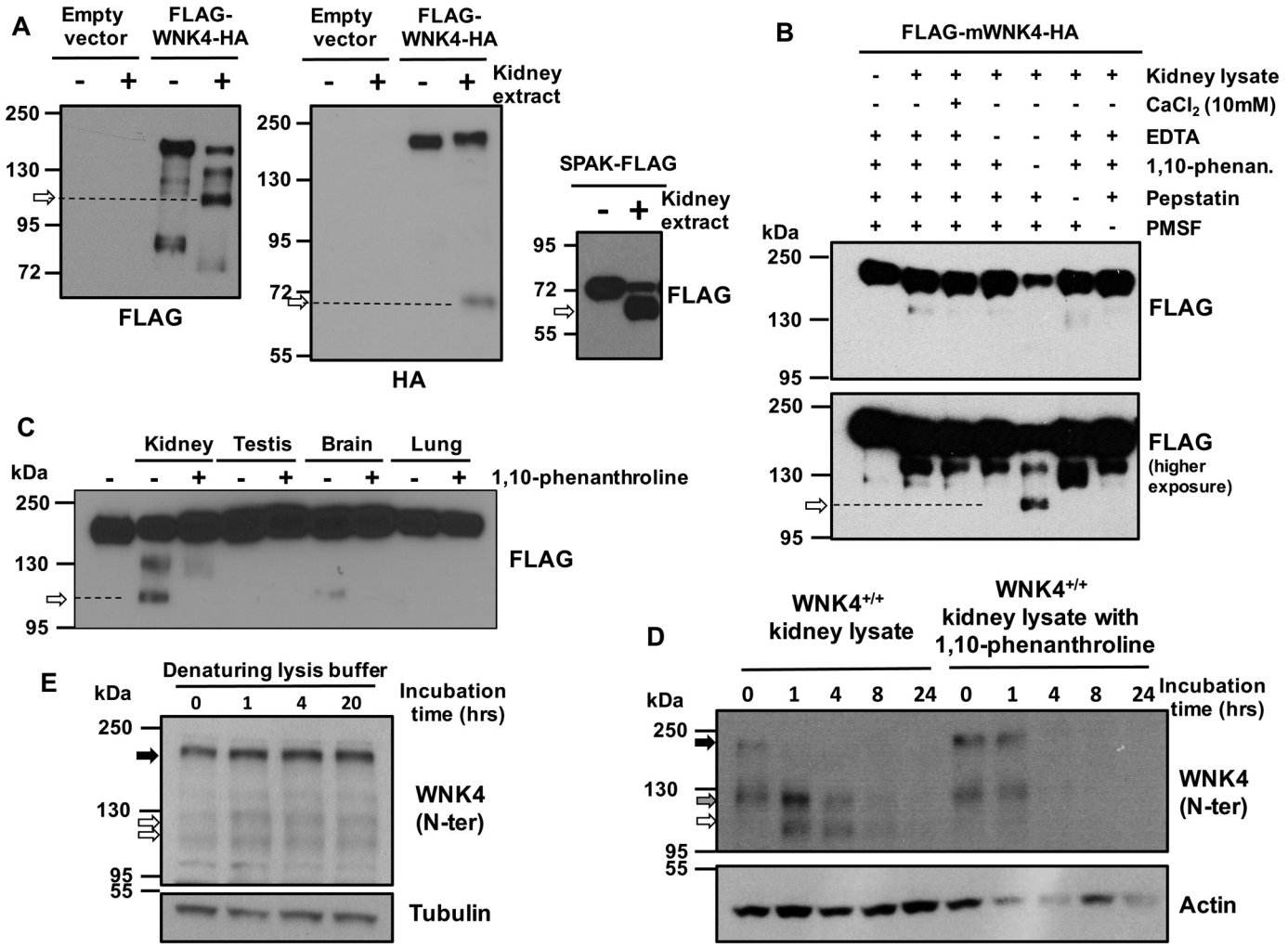

Figure 4. At least one of the short WNK4 variants observed in kidney lysates may be produced by a proteolytic event. *A*, FLAG-WNK4-HA (N- and C-terminal tags) and SPAK-FLAG (C-terminal tag) were immunopurified from HEK293 lysates and incubated with kidney lysates (70 mg) at 37 °C for 1.5 h. Western blots were performed with FLAG and HA antibodies as indicated. In the samples treated with kidney lysate, a decrease in the amount of full-length WNK4 and SPAK was observed, and a lower-sized band became apparent (*white arrow*), presumably due to a proteolytic cleavage event. For WNK4, lower-sized bands were observed with both FLAG and HA antibodies, suggesting that these bands may correspond to the N-terminal and C-terminal proteolytic fragments, respectively. This observation was reproducible in more than 10 independent experiments, some of which are presented in the following *panels* and in Fig. 5. *B*, proteolytic assays were performed as described in *A* in the presence of different protease inhibitors: phenylmethylsulfonyl fluoride (1 mM), pepstatin A (10 μM), EDTA (1 mM), and 1,10-phenanthroline (5 mM). The proteolytic event was only observed in the absence of 1,10-phenanthroline (indicated by a *white arrow*), suggesting that the protease responsible of this cleavage is Zn^{2+}-dependent. The same observation was made in two independent experiments. *C*, proteolytic assays performed as described in *A* with lysates of different tissues. WNK4 cleavage is more prominent using kidney lysate (indicated by a *white arrow*). Four independent assays were performed with similar results. *D*, incubation of kidney lysates at room temperature promotes an increase in the abundance of the shortest WNK4 fragment (*white arrow*). This is prevented by the addition of 1,10-phenanthroline (5 mM). Other forms of WNK4 are indicated by *black* and *gray arrows*. Three independent assays were performed with similar results. WNK4 antibody A was used. *E*, a kidney lysate was prepared by immediate homogenization of frozen tissue in lysis buffer containing 1% SDS, which prevents all enzymatic activity. The short WNK4 variants were detected (*white arrows*), suggesting that they are not artificially produced during tissue lysis. WNK4 antibody A was used.

databases from mouse kidney RNA-Seq studies (GEO accession numbers GSE79443 (31) and GSE81055). Only one alternative transcript was found that lacks exons 14 and 15 (Fig. S4). This transcript, however, could not explain the short WNK4 variants that we observe in kidney lysates, because it would produce a protein containing a portion of the C-terminal domain that is absent in the short variants that we detect (Fig. 1).

We hypothesized that the short WNK4 variants could be produced by proteolytic events. Full-length WNK4 carrying a FLAG and HA epitopes at the N and C termini, respectively, was produced in HEK293 cells. Following immunopurification, FLAG-WNK4-HA was incubated with 70 μg of kidney lysate at 37 °C for 1.5 h. Incubation with kidney lysate reduced the amount of full-length WNK4 detected with the FLAG antibody and produced a smaller band that ran between the 95 and 130 kDa markers (Fig. 4*A*). When probed with the HA antibody, a smaller band of approximately 70 kDa was also observed in the presence of kidney lysate (Fig. 4*A*). These small bands may correspond to the N-terminal and C-terminal proteolytic fragments, respectively. They were not detected in the lysate samples in the absence of FLAG-WNK4-HA (Fig. 4*A*), ruling them out as nonspecific bands recognized in the kidney lysate by these antibodies. As control, a SPAK proteolytic assay was performed in parallel using immunopurified SPAK-FLAG (C-terminal tag), and the previously reported proteolytic event was clearly observed (29).

To assess which type of protease is responsible for the cleavage, FLAG-WNK4-HA proteolytic assays were carried out in the presence of multiple combinations of protease inhibitors. The proteolytic event was only observed in the reaction lacking EDTA and 1,10-phenanthroline (Fig. 4*B*) and was not observed in the reaction containing EDTA and 1,10-phenanthroline in which Ca^{2+} was added in a concentration that exceeds the chelating capacity of EDTA (32). Moreover, previous reactions in which WNK4 cleavage was observed were carried out in the presence of the protease inhibitor mixture Complete (Roche Applied Science), which contains EDTA at low concentrations that are sufficient to chelate Ca^{2+} but not Zn^{2+} ions due to the lower affinity against the latter. These observations suggest that, similar to what was reported for SPAK (29), the protease responsible for the cleavage of WNK4 is probably a Zn^{2+}-dependent metalloprotease.

When lysates from different tissues were tested, the 1,10-phenanthroline–sensitive cleavage of WNK4 was noticeably more prominent upon incubation with kidney lysate than with other lysates (Fig. 4*C*). This is consistent with the expression pattern of the WNK4 short variants reported in Fig. 1*C*.

We then tested whether the proteolytic activity could be observed in endogenous WNK4 of mouse kidney lysates. Lysates were freshly prepared, and, immediately after homogenization, the lysate was split in two, and 1,10-phananthroline was added to one of the tubes. Aliquots were then prepared from each tube that were incubated at 25 °C for the indicated amounts of time (Fig. 4*D*). In the absence of 1,10-phenanthroline, a decrease in the full-length band was observed after only 1 h of incubation, and, at this time point, the abundance of the band of lowest size already increased with respect to time 0 (Fig. 4*D*). This increase was not observed in the lysates treated with 1,10-phenanthroline, suggesting that the band of lowest size was generated by a proteolytic cleavage mediated by a Zn^{2+}-dependent protease. Generalized protein degradation was also observed, which explains the absence of band detection in the final time points.

Finally, given the observations just mentioned, we wanted to rule out the possibility that the short WNK4 bands observed in blots were produced as an artifact during lysate preparation, because this would mean that the short variants of WNK4 do not really exist within intact renal cells. To do this, a kidney lysate was prepared by immediate homogenization of frozen tissue in lysis buffer containing 1% SDS (33). This lysis method prevents all enzymatic activity. The short WNK4 variants were detected in this lysate (Fig. 4*E*), suggesting that they are not artificially produced during tissue lysis when WNK4 proteins come in contact with extracellular proteases or other proteases present in cell types that lack WNK4 expression.

Renal WNK4 short variants probably lack a SPAK-binding site and may be unable to phosphorylate SPAK

WNK4 *in vitro* proteolytic reactions were run in parallel to kidney lysates from $WNK4^{+/+}$ and $WNK4^{-/-}$ mice to compare the electrophoretic mobility of the WNK4 N-terminal fragment produced in proteolytic assays with that of the short WNK4 variants observed in lysates. Proteolytic reactions were performed using kidney lysates from $WNK4^{-/-}$ mice. This allowed us to use an antibody directed against a WNK4 N-terminal epitope to detect the proteolytic fragments without detecting any WNK4 signal from the lysates used for the proteolytic reaction. We observed that the WNK4 N-terminal proteolytic fragment runs at a height similar to that of the shortest WNK4 variant observed in $WNK4^{+/+}$ kidney lysates (Fig. 5*A*). We then compared the electrophoretic mobility of the different variants of WNK4 observed in kidney lysates with that of several WNK4 mutant constructs truncated at the C terminus. The full-length WNK4 expressed in HEK293 cells presented an electrophoretic mobility similar to that of the full-length WNK4 observed in kidney lysates (Fig. 5*B*). The next WNK4 band observed in kidney lysates (the middle band) ran at a similar height as the WNK4-L866X mutant, and the shortest WNK4 kidney band ran faster than the WNK4-L866X mutant and slower than the WNK4-V740X mutant. Thus, assuming that the mobility of the renal WNK4 variants is not affected by an unknown modification or factor that is absent in HEK293 cells, or vice versa, we can conclude that the short renal WNK4 variants probably lack the C-terminal SPAK-binding motif (residues 996–999). According to the results presented in Fig. 2*B*, this would render them unable to phosphorylate SPAK.

Finally, with the purpose of narrowing down the segment of the protein containing the site in which WNK4 is cleaved *in vitro*, and probably *in vivo*, we generated new WNK4 mutants harboring deletions of different portions of the C terminus (Fig. 5*C*). We hypothesized that the *in vitro* cleavage would not be observed with the mutant lacking the cleavage site. As expected, all but one of the five deletion mutants were cleaved in *in vitro* proteolytic reactions, and cleavage was prevented by the addition of 1,10-phenanthroline (Fig. 5*D*). We failed to observe cleavage of the WNK4-Δ740–781 mutant, suggesting that the cleavage site may be present within the segment flanked by residues 740–781. Consistent with this conclusion, all three mutants harboring deletions of segments located downstream of the putative cleavage region produced N-terminal proteolytic fragments of a similar size to the one observed with the WNK4-WT. In contrast, the WNK4-Δ601–739 mutant produced an N-terminal proteolytic fragment of smaller size, presumably because in this mutant, the cleavage site is located downstream of the deletion, and thus the 601–739 region is normally located within the N-terminal proteolytic fragment.

Abundance of short WNK4 variants is not altered by changes in dietary Na^+ and K^+ content

Given that modifications in the dietary content of Na^+ and K^+ affect the activity of NCC and other targets of regulation of WNK4 (like ROMK and ENaC), we decided to test whether these dietary modifications could also affect the abundance of WNK4 isoforms, rationalizing that this could have an impact on the activity of the downstream targets. No changes were observed with the low-Na^+ diet, and an increase in the abundance of all isoforms was observed in mice given a low-K^+ diet (Fig. 6, *A* and *B*). The latter result is consistent with a previous report (34), and the changes observed are probably due to a decrease in KLHL3–CUL3-RING–mediated WNK4 degradation. However, no changes in the relative abundance

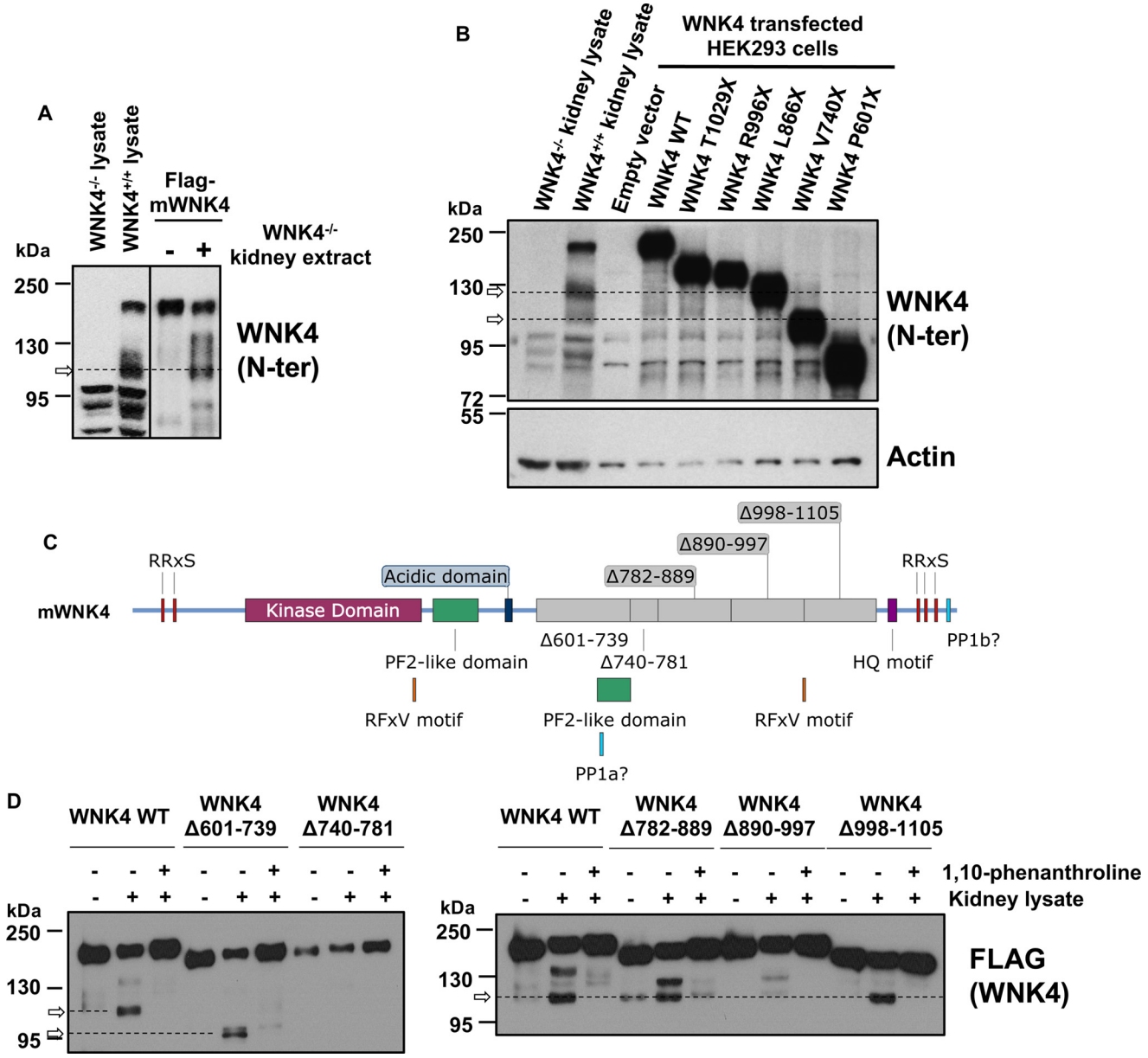

Figure 5. Size analysis of WNK4 short variants. *A*, Western blotting of WNK4$^{+/+}$ and WNK4$^{-/-}$ kidney lysates run in parallel with WNK4 proteolytic reactions (performed as in Fig. 4*A*, but using kidney lysates from WNK4$^{-/-}$ mice) to compare the electrophoretic mobility of the WNK4 fragments with that of the short band that is product of the *in vitro* proteolytic cleavage (*white arrow*). For clarity, the blot image was split in two to present two different film exposure times. Three independent experiments were performed. WNK4 antibody A was used. *B*, Western blotting of WNK4$^{+/+}$ and WNK4$^{-/-}$ kidney lysates run in parallel with lysates of HEK293 cells transfected with different truncated WNK4 mutants. WNK4 antibody A was used. The electrophoretic mobility of the renal WNK4 short variants (*white arrows*) suggests that they may be around 740–866 amino acids long and might lack a SPAK-binding site. *C*, *schematic representation* of WNK4 constructs in which different segments were deleted to narrow down the region containing the cleavage site in WNK4. *D*, proteolytic assays performed with different WNK4 constructs harboring deletions in the C-terminal region. All constructs were cleaved upon incubation with kidney lysate (proteolytic fragment indicated by the *white arrow*), except for the one that lacks residues 740–782. This suggests that the cleavage site might be located within this segment of the protein. Four independent experiments were performed.

of WNK4 forms were observed, suggesting that the cleavage of WNK4 is not regulated in response to these dietary manipulations.

Finally, given that it is clear that WNK4 plays an important role in DCT physiology, we decided to analyze the expression of the WNK4 short variants in samples from DCT tubules isolated by COPAS^{TM}. Indeed, we were able to observe at least one of the short variants in these samples. Due to the low signal detected, it was unclear whether the second short variant is expressed in DCT cells.

Discussion

Kidney-specific isoforms of the kinases WNK1 and SPAK have been described. These isoforms present functional properties that differ from those of the full-length proteins (28, 35). Hence, their characterization has been important to understand the molecular pathways implicated in the regulation of renal salt transport. Similarly, the characterization of the WNK4 short variants described in this work may be important to gain a more accurate understanding of WNK4's role in kidney physiology.

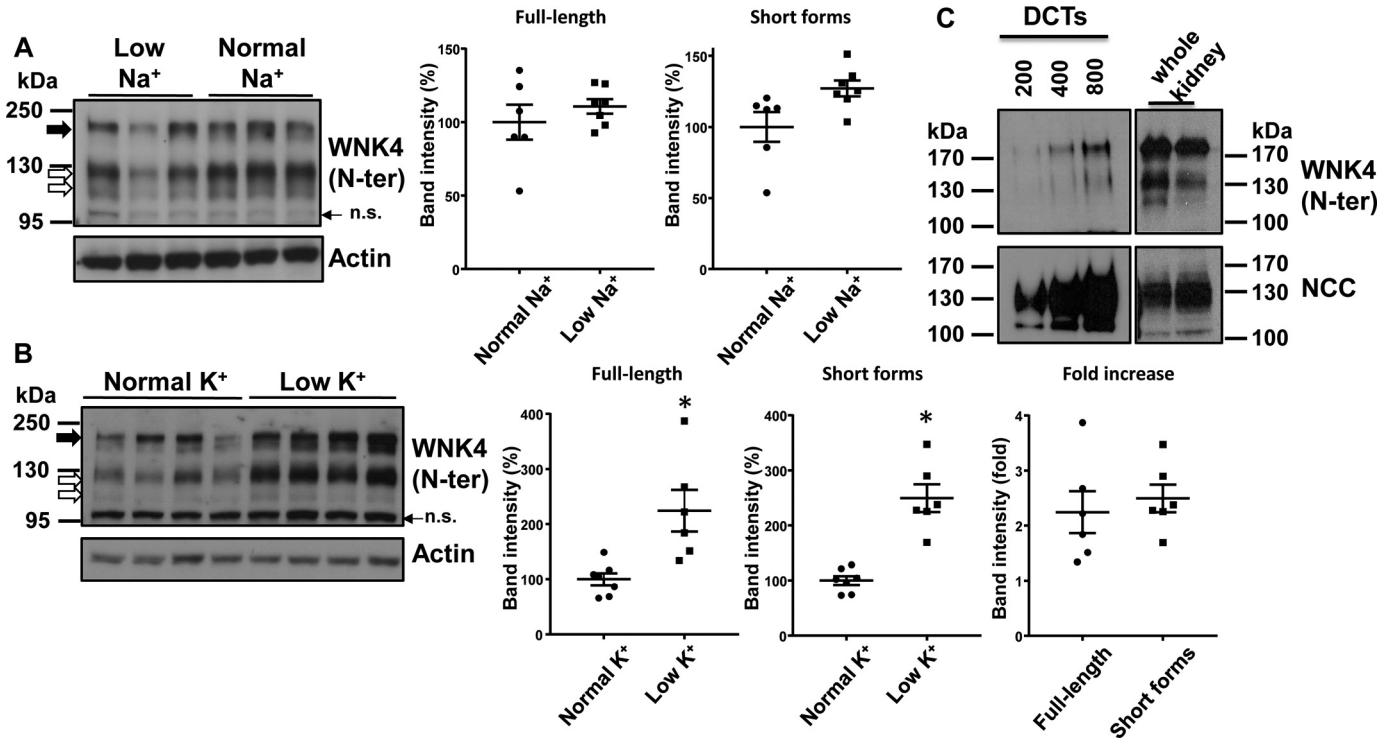

Figure 6. Effect of changes in dietary electrolyte intake on the abundance of renal WNK4 forms. *A*, WT C57Bl/6 mice were given normal Na^+ diet ($n = 6$) or low Na^+ diet ($n = 7$) for a period of 4 days. Kidney lysates were prepared and WNK4 Western blots were performed with an antibody directed against an N-terminal epitope (antibody A) (41). The full-length form is indicated with a *black arrow*. Short WNK4 variants are indicated with *white arrows*. *n.s.*, nonspecific bands. Results of quantitation of band intensities for the full-length and short forms of WNK4 are presented. Data are mean ± S.E. (*error bars*). *B*, same as in *A*, but mice were fed with normal or low-K^+ diets for 7 days ($n = 6$ for each group). Results of quantitation of band intensities for the full-length and short forms of WNK4 are presented. Data are mean ± S.E. *, $p < 0.01$ *versus* normal K^+. No apparent shift in the relative abundance of WNK4 forms was observed with any of these dietary manipulations. *C*, DCTs were enriched by COPAS (43) and then subjected to Western blot analysis. At least one of the short WNK4 fragments was observed. NCC blot was performed to confirm DCT enrichment.

Here, we used multiple antibodies for Western blotting assays and LC-MS/MS studies, which helped us to confirm that indeed short fragments of WNK4 are present in kidney lysates that lack a portion of the C-terminal domain (Fig. 1 and Fig. S1).

Given that alternative WNK4 transcripts that could explain the short WNK4 variants were not observed, we tested the possibility that they could be the product of a proteolytic event. Indeed, we observed that kidney lysates appear to possess proteolytic activity toward WNK4 and that this activity produces a band of a size similar to that of the shortest WNK4 variant observed *in vivo* (Figs. 4 and 5). This phenomenon was similar to the one characterized by Markadieu *et al.* (29) for the kinase SPAK: a proteolytic event giving rise to SPAK short variants that is observed upon incubation with kidney lysates, which was prevented by the addition of 1,10-phenanthroline, an inhibitor of Zn^{2+} metalloproteases (36). It remains unclear which is the protease responsible for the SPAK cleavage (37).

It should be noted that only one short WNK4 fragment was produced upon incubation of recombinant WNK4 with kidney lysates. Thus, the origin of only one of the two short WNK4 bands observed in kidney lysates may be explained by a proteolytic event. The second band may be the product of an alternative transcript that we failed to identify or the product of a proteolytic event that was not observed in the conditions tested.

Our experiments narrowed down the location of the cleavage site to a 41-residue-long segment of the protein (within residues 740–781) (Fig. 5). Cleavage in this region would produce a WNK4 fragment that would lack the C-terminal SPAK-binding site (26) and the HQ motif that is important for WNK homo- or heterodimerization (23, 24). The same would be true for the second short variant of larger size observed in kidney, based on its electrophoretic mobility. Thus, these short variants may be unable to autophosphorylate and to phosphorylate SPAK, so one possibility is that their generation may be a mechanism to inactivate the pathway. Another possibility is that they may play a role in the kinase activity-independent regulation of targets like ENaC and ROMK (11, 12), or in the SPAK-independent regulation of Slc12 cotransporters (26). Because no shift in the abundance of WNK4 forms was observed in mice exposed to low-Na^+ or low-K^+ diets, it is not yet clear whether this process is regulated. Further research will be necessary to understand the physiological significance of the WNK4 short variants. Interestingly, it has been recently reported that Zn^{2+} deficiency in DCT cells and in mice is associated with an increase in NCC expression and activity (38). Although the mechanism is currently unknown, one possibility is that Zn^{2+} depletion in DCT cells may lead to decreased WNK4 and SPAK cleavage and, thus, NCC activation.

Finally, it has been recognized that the PP1 phosphatase is an important regulator of the WNK-SPAK/OSR1-Slc12 pathway. For instance, it was shown that inhibition of PP1 activity by calyculin A prevents the activation of KCCs that is observed in the presence of kinase-inactive WNK3 (39) and inhibits the

activity of KCC4 observed in hypotonic conditions (40). Later, Lin *et al.* described two motifs within WNK4 that harbor the consensus sequence required for interaction with PP1, and they showed that elimination of these motifs prevents WNK4–PP1 co-immunoprecipitation (21). More recently, Frenette-Cotton *et al.* (40) showed that mutation of both of these motifs prevents WNK4's ability to inhibit KCC4, and, thus, they proposed that WNK4 inhibits PP1 activity, which translates into KCC4 down-regulation.

In the present work, the study of the short variants of WNK4 has led us to a more comprehensive characterization of the putative PP1-binding sites in WNK4. By directly analyzing the ability of the WNK4–PP1 binding mutants to phosphorylate SPAK and their phosphorylation levels in the presence of PP1, we have obtained robust results showing that PP1α and PP1γ are strong regulators of WNK4 activity by promoting WNK4 dephosphorylation (Fig. 3). We also observed that only the second K*X*V*X*F motif present in WNK4 (here termed PP1b) is necessary for PP1-mediated regulation of WNK4. Elimination of this site turned WNK4 into a constitutively active kinase, suggesting that WNK4 activity depends on the balance between phosphorylating stimuli (*e.g.* low intracellular chloride (14) or increased angiotensin II (16)) and dephosphorylating stimuli through PP1α and PP1γ. Of note, these results fit well with our previous description of a "negative signal regulatory domain" in WNK4 that comprises the terminal 50 residues of the protein (18).

Regarding the first K*X*V*X*F motif (PP1a), we show that it may not function as a PP1-binding site, because elimination of this site does not alter PP1-mediated WNK4 dephosphorylation. Instead, mutation of this site ablates WNK4 activity, even in the context of the high levels of WNK4 phosphorylation observed when both sites are mutated together (Fig. 3). Thus, we hypothesize that this loss of activity is due to disruption of a domain that is functionally important. Indeed, the PP1a site lies within a region of WNK4 that has been predicted to have a PF2-like fold similar to the one present in SPAK and OSR1. In these kinases, the PF2 domain constitutes the binding site for RFXV motifs present in WNK kinases and Slc12 transporters. Thus, although we cannot yet ascribe a particular role for this domain in WNK4, we can argue that the PP1a motif probably does not constitute a PP1-binding site. From this perspective, the results of Frenette-Cotton *et al.* (40) acquire a different interpretation; WNK4 is not a regulator of PP1, but instead, PP1 regulates WNK4 activity, and the observation that the WNK4 mutant with both putative PP1-binding sites eliminated is unable to inhibit KCC4 may be explained by the fact that this is a mutant that is unable to phosphorylate SPAK.

In conclusion, we have identified C-terminally truncated, kidney-specific, short variants of the kinase WNK4. At least one of these short variants appears to be a product of a proteolytic event, and our experiments suggest that they both probably lack a SPAK-binding site and an HQ motif. Thus, they are probably inactive, and their physiological relevance remains to be determined. Finally, this work has led us to the identification of a *bona fide* PP1-binding site in WNK4, which is located within the last 12 amino acid residues of the kinase. We have shown that PP1 regulates WNK4 phosphorylation levels and, thus, WNK4 activity.

Experimental procedures

Mouse studies

Animal studies were approved by the animal care and use committees of our institutions. Most studies were performed in male WT C57BL/6 mice (age 12–16 weeks). WNK4-knockout mice and WNK4-PHAII transgenic mice were also used (C57BL/6 background) (4, 8). Teklad custom normal diet (containing 0.49% NaCl; TD.96208) and NaCl-deficient diet (TD.90228) were given for 4 days (8). Low-K^+ (0% K^+) diet was obtained from TestDiet (St. Louis, MO), whereas normal K^+ was prepared by adding KCl to make a 1.2% K^+ diet. Mice were given these modified diets for 7 days before being sacrificed.

Western blots

Tissues were snap-frozen in liquid nitrogen and later homogenized (250 mM sucrose, 10 mM triethanolamine, 1× protease inhibitors (Roche Applied Science), 1× phosphatase inhibitors (Sigma)). Protein concentration was determined by the BCA protein assay (Pierce). Protein extracts were subjected to SDS-PAGE and transferred to polyvinylidene difluoride membranes. Membranes were blocked for 1 h in 10% (w/v) nonfat milk dissolved in TBS-Tween 20 (TBSt). Antibodies were diluted in TBSt containing 5% (w/v) nonfat milk. Membranes were incubated with primary antibodies overnight at 4 °C and with HRP-coupled secondary antibodies at 25 °C for 1 h. Signals were detected with enhanced chemiluminescence reagent. Immunoblots were developed using film.

The following antibodies were used: WNK4 (N-terminal epitope, raised in rabbit, generated by Dr. David H. Ellison's group (41), antibody A); tubulin (Sigma, T5168, raised in mouse); actin (Santa Cruz Biotechnology, Inc., sc-1616 HRP, raised in goat); HA (Sigma, H6533, raised in mouse); FLAG (Sigma, A8592, raised in mouse); pRRXS (Cell Signaling, 9624 (16), raised in rabbit); sheep-HRP (Jackson Immunoresearch); and rabbit-HRP (Jackson Immunoresearch). Several antibodies were obtained from the Medical Research Council phosphorylation unit at Dundee University (all are polyclonal antibodies raised in sheep): WNK4 (C-terminal epitope, S064B (8), antibody B); WNK4 (N-terminal epitope, S121B (41), antibody C); pSPAK-Ser-373 (S670B) (42); and NCC (S965B) (8). The specificity of all antibodies used has been previously tested.

COPAS

Isolation of DCT has been described previously (43). Briefly, mice expressing enhanced GFP under the PV promoter were anesthetized and perfused with ice-cold Krebs buffer. Kidney cortex was finely minced before incubation in digestion solution (1 mg/ml collagenase type 1 and 2,000 units/ml hyaluronidase in Krebs buffer, pH 7.3) for 15 min at 37 °C. Tubules collected from digestion reactions were placed on ice and sorted by the COPAS. Each suspension of fluorescent tubules was collected in a 1.5-ml Eppendorf tube, previously coated with 0.5% (w/v) BSA in PBS/NaOH, pH 7.4. Tubules were lysed with Laemmli buffer.

Mass spectrometry

Mouse kidney lysates were prepared as described above. For WNK4 immunoprecipitation, 1 mg of lysate was incubated with 10 μg of sheep anti-WNK4 antibody (MRC Dundee S121B) (23) and Protein A/G magnetic beads (Pierce) for 2 h at 4 °C. Beads were washed five times with a buffer containing 0.025 M Tris, pH 7.4, 0.15 M NaCl, 0.001 M EDTA, 1% Nonidet P40, 5% glycerol. Bound proteins were eluted by incubation in glycine buffer, pH 2, for 10 min and then prepared for SDS-PAGE. Bands were excised from the gel and processed at the MS and Proteomics Resource at Yale. Briefly, on a tilt table, the gel band was washed with 1) 250 μl of 50% acetonitrile for 5 min, followed by 2) 250 μl of 50% acetonitrile containing 50 mM NH_4HCO_3 for 10–30 min, and then finally with 3) 250 μl of 50% acetonitrile containing 10 mM NH_4HCO_3 for 10–30 min. The final wash was removed, and the gel was SpeedVac-dried. 60 μl of a 1:15 dilution of a 0.1 mg/ml trypsin stock solution was added to the gel and allowed to absorb for 10 min. An additional volume of 10 mM NH_4HCO_3 was added to cover the gel pieces and then incubated at 37 °C for 18 h. Peptides were then extracted by adding 250 μl of 0.1% TFA, 80% acetonitrile and shaking for 30 min. Extract was transferred to a new tube and dried. Dried peptide pellet was dissolved in 70% formic acid, diluted with 0.1% TFA, and finally subjected to LC-MS/MS analysis using the LTQ Orbitrap XL that is equipped with a Waters nanoACQUITY UPLC system and uses a Waters Symmetry C18 180 μm × 20-mm trap column and a 1.7 μm, 75 μm × 250-mm nanoACQUITY UPLC column for peptide separation. The acquired data were peak-picked and searched using the Mascot Distiller and the Mascot search algorithm, respectively. Protein identification was achieved using the Mascot search algorithm (Matrix Science) as described (44), and MS spectral features were searched against the SWISSPROT Mouse database along with a user-generated WNK4 protein database.

Cell culture

HEK293 cells (ATCC® CRL-1573) were used for transient transfection of mWNK4-HA, FLAG-mWNK4 (16), HA-SPAK, SPAK-FLAG (FLAG inserted in the C-terminal by FastCloning (45)), and FLAG-PP1-α, -β, and -γ (kindly provided by Dr. Jeremy Nichols) (46). Cells were grown to 70–80% confluence and transfected with Lipofectamine 2000 (Life Technologies, Inc.). Mutations were introduced into the WNK4 clone by site-directed mutagenesis using Phusion® high-fidelity DNA polymerase (New England Biolabs) and confirmed by Sanger sequencing. Deletions were performed by FastCloning (45). 48 h after transfection, cells were lysed with a lysis buffer containing 50 mM Tris·HCl (pH 7.5), 1 mM EGTA, 1 mM EDTA, 50 mM sodium fluoride, 5 mM sodium pyrophosphate, 1 mM sodium orthovanadate, 1% (w/v) Nonidet P-40, 270 mM sucrose, 0.1% (v/v) 2-mercaptoethanol, and protease inhibitors (Complete tablets; Roche Applied Science), and protein concentration was quantified.

In vitro proteolytic assays

Recombinant FLAG-mWNK4-HA was immunoprecipitated using a FLAG® Immunoprecipitation Kit (FLAGIPT1, Sigma). After washing the beads, 70 μg of kidney lysate (prepared with lysis buffer containing 125 mM NaCl, 10% glycerol, 1 mM EGTA, 1 mM EDTA, 1 mM phenylmethylsulfonyl fluoride, 10 μM leupeptin, 4 μM aprotinin, 10 μM pepstatin, 1% Triton X-100, 0.5% SDS, 20 mM HEPES, pH 7.4) was added to the beads and incubated for 90 min at 37 °C (final reaction volume of 30 μl in 50 mM HEPES, 140 mM NaCl, pH 7.4, with protease inhibitors as indicated). Reactions were stopped by adding Laemmli buffer and heating at 95 °C for 10 min. Eluates were used for Western blotting assays.

Statistical analysis

For comparison between two groups, unpaired Student's *t* test (two-tailed) was used. For comparison between multiple groups, analysis of variance tests were performed, followed by Tukey post hoc tests. A difference between groups was considered significant when $p < 0.05$.

Na^+ uptake experiments

The use of *X. laevis* frogs was approved by our institutional committee on animal research. NCC activity was assessed in *X. laevis* oocytes microinjected with NCC cRNA alone or together with WT WNK4 or WNK4-T1029X. Two days post-injection, the thiazide-sensitive Na^+ uptake was assessed as described previously (9). Briefly, $^{22}Na^+$ tracer uptake was assessed in groups of 10–15 oocytes. A 30-min incubation at 32 °C in a Cl^--free ND96 medium containing 1 mM ouabain, 0.1 mM amiloride, and 0.1 mM bumetanide was followed by a 60-min uptake period in a K^+-free NaCl medium (40 mM NaCl, 56 mM sodium gluconate, 4.0 mM $CaCl_2$, 1.0 mM $MgCl_2$, and 5.0 mM HEPES, pH 7.4) containing ouabain, amiloride, bumetanide, and 2 μCi of $^{22}Na^+$/ml. Oocytes were washed five times in ice-cold uptake solution to remove tracer in the extracellular fluid. Individual oocytes were dissolved in 10% SDS, and the tracer activity was determined for each oocyte by β-scintillation counting.

Author contributions—A. R. M.-d.-O., C.-L. Y., D. E., G. G., and M. C. B. conceptualization; A. R. M.-d.-O., K. L. S., C.-L. Y., and M. C. B. formal analysis; A. R. M.-d.-O., A. R.-G., S. B.-V., K. L.-R., N. V., D. P.-A., I. A. D.-L. R.-V., A. W., K. L. S., J. Z., C.-L. Y., and M. C. B. investigation; A. R. M.-d. O., I. A. D.-L. R.-V., and M. C. B. visualization; A. R. M.-d. O., I. A. D.-L. R.-V., J. L., and M. C. B. methodology; A. R. M.-d. O., G. G., and M. C. B. writing-original draft; A. W. and J. L. resources; R. P. L., C.-L. Y., D. E., G. G., and M. C. B. supervision; R. P. L., C.-L. Y., D. E., G. G., and M. C. B. funding acquisition; M. C. B. project administration; M. C. B. writing-review and editing.

Acknowledgments—We thank Dr. Jeremy Nichols (Parkinson's Institute and Clinical Center, Sunnyvale, CA) for kindly providing the PP1 clones. We also thank Mary LoPresti, Jean Kanyo, and Dr. TuKiet Lam from the MS and Proteomics Resource at Yale University for assistance in the MS sample preparation, data collection, and MS methodology write-up, respectively.

References

1. Kahle, K. T., Gimenez, I., Hassan, H., Wilson, F. H., Wong, R. D., Forbush, B., Aronson, P. S., and Lifton, R. P. (2004) WNK4 regulates apical and

basolateral Cl^- flux in extrarenal epithelia. *Proc. Natl. Acad. Sci. U.S.A.* **101,** 2064–2069 CrossRef Medline
2. Wilson, F. H., Disse-Nicodème, S., Choate, K. A., Ishikawa, K., Nelson-Williams, C., Desitter, I., Gunel, M., Milford, D. V., Lipkin, G. W., Achard, J. M., Feely, M. P., Dussol, B., Berland, Y., Unwin, R. J., Mayan, H., *et al.* (2001) Human hypertension caused by mutations in WNK kinases. *Science* **293,** 1107–1112 CrossRef Medline
3. Grimm, P. R., Coleman, R., Delpire, E., and Welling, P. A. (2017) Constitutively active SPAK causes hyperkalemia by activating NCC and remodeling distal tubules. *J. Am. Soc. Nephrol.* **28,** 2597–2606 CrossRef Medline
4. Lalioti, M. D., Zhang, J., Volkman, H. M., Kahle, K. T., Hoffmann, K. E., Toka, H. R., Nelson-Williams, C., Ellison, D. H., Flavell, R., Booth, C. J., Lu, Y., Geller, D. S., and Lifton, R. P. (2006) Wnk4 controls blood pressure and potassium homeostasis via regulation of mass and activity of the distal convoluted tubule. *Nat. Genet.* **38,** 1124–1132 CrossRef Medline
5. Zhang, C., Wang, L., Su, X.-T., Zhang, J., Lin, D.-H., and Wang, W.-H. (2016) ENaC and ROMK activity are inhibited in the DCT2/CNT of TgWnk4PHAII mice. *Am. J. Physiol. Renal Physiol.* **312,** F622–F688
6. Shibata, S., Zhang, J., Puthumana, J., Stone, K. L., and Lifton, R. P. (2013) Kelch-like 3 and Cullin 3 regulate electrolyte homeostasis via ubiquitination and degradation of WNK4. *Proc. Natl. Acad. Sci. U.S.A.* **110,** 7838–7843 CrossRef Medline
7. Wakabayashi, M., Mori, T., Isobe, K., Sohara, E., Susa, K., Araki, Y., Chiga, M., Kikuchi, E., Nomura, N., Mori, Y., Matsuo, H., Murata, T., Nomura, S., Asano, T., Kawaguchi, H., Nonoyama, S., Rai, T., Sasaki, S., and Uchida, S. (2013) Impaired KLHL3-mediated ubiquitination of WNK4 causes human hypertension. *Cell Rep.* **3,** 858–868 CrossRef Medline
8. Castañeda-Bueno, M., Cervantes-Pérez, L. G., Vázquez, N., Uribe, N., Kantesaria, S., Morla, L., Bobadilla, N. A., Doucet, A., Alessi, D. R., and Gamba, G. (2012) Activation of the renal Na^+:Cl^- cotransporter by angiotensin II is a WNK4-dependent process. *Proc. Natl. Acad. Sci. U.S.A.* **109,** 7929–7934 CrossRef Medline
9. Pacheco-Alvarez, D., Cristóbal, P. S., Meade, P., Moreno, E., Vazquez, N., Muñoz, E., Díaz, A., Juárez, M. E., Giménez, I., and Gamba, G. (2006) The Na^+:Cl^- cotransporter is activated and phosphorylated at the amino-terminal domain upon intracellular chloride depletion. *J. Biol. Chem.* **281,** 28755–28763 CrossRef Medline
10. Richardson, C., Rafiqi, F. H., Karlsson, H. K. R., Moleleki, N., Vandewalle, A., Campbell, D. G., Morrice, N. A., and Alessi, D. R. (2008) Activation of the thiazide-sensitive Na^+-Cl^- cotransporter by the WNK-regulated kinases SPAK and OSR1. *J. Cell Sci.* **121,** 675–684 CrossRef Medline
11. Kahle, K. T., Wilson, F. H., Leng, Q., Lalioti, M. D., O'Connell, A. D., Dong, K., Rapson, A. K., MacGregor, G. G., Giebisch, G., Hebert, S. C., and Lifton, R. P. (2003) WNK4 regulates the balance between renal NaCl reabsorption and K^+ secretion. *Nat. Genet.* **35,** 372–376 CrossRef Medline
12. Ring, A. M., Cheng, S. X., Leng, Q., Kahle, K. T., Rinehart, J., Lalioti, M. D., Volkman, H. M., Wilson, F. H., Hebert, S. C., and Lifton, R. P. (2007) WNK4 regulates activity of the epithelial Na^+ channel *in vitro* and *in vivo*. *Proc. Natl. Acad. Sci. U.S.A.* **104,** 4020–4024 CrossRef Medline
13. Piala, A. T., Moon, T. M., Akella, R., He, H., Cobb, M. H., and Goldsmith, E. J. (2014) Chloride sensing by WNK1 involves inhibition of autophosphorylation. *Sci. Signal.* **7,** ra41 CrossRef Medline
14. Bazúa-Valenti, S., Chávez-Canales, M., Rojas-Vega, L., González-Rodríguez, X., Vázquez, N., Rodríguez-Gama, A., Argaiz, E. R., Melo, Z., Plata, C., Ellison, D. H., García-Valdés, J., Hadchouel, J., and Gamba, G. (2015) The effect of WNK4 on the Na^+-Cl^- cotransporter is modulated by intracellular chloride. *J. Am. Soc. Nephrol.* **26,** 1781–1786 CrossRef Medline
15. Terker, A. S., Zhang, C., McCormick, J. A., Lazelle, R. A., Zhang, C., Meermeier, N. P., Siler, D. A., Park, H. J., Fu, Y., Cohen, D. M., Weinstein, A. M., Wang, W. H., Yang, C. L., and Ellison, D. H. (2015) Potassium modulates electrolyte balance and blood pressure through effects on distal cell voltage and chloride. *Cell Metab.* **21,** 39–50 CrossRef Medline
16. Castañeda-Bueno, M., Arroyo, J. P., Zhang, J., Puthumana, J., Yarborough, O., 3rd, Shibata, S., Rojas-Vega, L., Gamba, G., Rinehart, J., and Lifton, R. P. (2017) Phosphorylation by PKC and PKA regulate the kinase activity and downstream signaling of WNK4. *Proc. Natl. Acad. Sci. U.S.A.* **114,** E879–E886 CrossRef Medline
17. San-Cristobal, P., Ponce-Coria, J., Vázquez, N., Bobadilla, N. A., and Gamba, G. (2008) WNK3 and WNK4 amino-terminal domain defines their effect on the renal Na^+-Cl^- cotransporter. *Am. J. Physiol. Renal Physiol.* **295,** F1199–F1206 CrossRef Medline
18. Yang, C. L., Zhu, X., Wang, Z., Subramanya, A. R., and Ellison, D. H. (2005) Mechanisms of WNK1 and WNK4 interaction in the regulation of thiazide-sensitive NaCl cotransport. *J. Clin. Invest.* **115,** 1379–1387 CrossRef Medline
19. Ring, A. M., Leng, Q., Rinehart, J., Wilson, F. H., Kahle, K. T., Hebert, S. C., and Lifton, R. P. (2007) An SGK1 site in WNK4 regulates Na^+ channel and K^+ channel activity and has implications for aldosterone signaling and K^+ homeostasis. *Proc. Natl. Acad. Sci. U.S.A.* **104,** 4025–4029 CrossRef Medline
20. Gagnon, K. B., and Delpire, E. (2012) Molecular physiology of SPAK and OSR1: two Ste20-related protein kinases regulating ion transport. *Physiol. Rev.* **92,** 1577–1617 CrossRef Medline
21. Lin, D.-H., Yue, P., Rinehart, J., Sun, P., Wang, Z., Lifton, R., and Wang, W.-H. (2012) Protein phosphatase 1 modulates the inhibitory effect of With-no-Lysine kinase 4 on ROMK channels. *Am. J. Physiol. Renal Physiol.* **303,** F110–F119 CrossRef Medline
22. Piechotta, K., Lu, J., and Delpire, E. (2002) Cation chloride cotransporters interact with the stress-related kinases Ste20-related proline-alanine-rich kinase (SPAK) and oxidative stress response 1 (OSR1). *J. Biol. Chem.* **277,** 50812–50819 CrossRef Medline
23. Thastrup, J. O., Rafiqi, F. H., Vitari, A. C., Pozo-Guisado, E., Deak, M., Mehellou, Y., and Alessi, D. R. (2012) SPAK/OSR1 regulate NKCC1 and WNK activity: analysis of WNK isoform interactions and activation by T-loop trans-autophosphorylation. *Biochem. J.* **441,** 325–337 CrossRef Medline
24. Chávez-Canales, M., Zhang, C., Soukaseum, C., Moreno, E., Pacheco-Alvarez, D., Vidal-Petiot, E., Castañeda-Bueno, M., Vázquez, N., Rojas-Vega, L., Meermeier, N. P., Rogers, S., Jeunemaitre, X., Yang, C. L., Ellison, D. H., Gamba, G., and Hadchouel, J. (2014) WNK-SPAK-NCC cascade revisited: WNK1 stimulates the activity of the Na-Cl cotransporter via SPAK, an effect antagonized by WNK4. *Hypertension* **64,** 1047–1053 CrossRef Medline
25. Wilson, F. H., Kahle, K. T., Sabath, E., Lalioti, M. D., Rapson, A. K., Hoover, R. S., Hebert, S. C., Gamba, G., and Lifton, R. P. (2003) Molecular pathogenesis of inherited hypertension with hyperkalemia: the Na-Cl cotransporter is inhibited by wild-type but not mutant WNK4. *Proc. Natl. Acad. Sci. U.S.A.* **100,** 680–684 CrossRef Medline
26. Ponce-Coria, J., Markadieu, N., Austin, T. M., Flammang, L., Rios, K., Welling, P. A., and Delpire, E. (2014) A novel Ste20-related proline/alanine-rich kinase (SPAK)-independent pathway involving calcium-binding protein 39 (Cab39) and serine threonine kinase with no lysine member 4 (WNK4) in the activation of Na-K-Cl cotransporters. *J. Biol. Chem.* **289,** 17680–17688 CrossRef Medline
27. Shi, Y. (2009) Serine/threonine phosphatases: mechanism through structure. *Cell* **139,** 468–484 CrossRef Medline
28. McCormick, J. A., Mutig, K., Nelson, J. H., Saritas, T., Hoorn, E. J., Yang, C. L., Rogers, S., Curry, J., Delpire, E., Bachmann, S., and Ellison, D. H. (2011) A SPAK isoform switch modulates renal salt transport and blood pressure. *Cell Metab.* **14,** 352–364 CrossRef Medline
29. Markadieu, N., Rios, K., Spiller, B. W., McDonald, W. H., Welling, P. A., and Delpire, E. (2014) Short forms of Ste20-related proline/alanine-rich kinase (SPAK) in the kidney are created by aspartyl aminopeptidase (Dnpep)-mediated proteolytic cleavage. *J. Biol. Chem.* **289,** 29273–29284 CrossRef Medline
30. Scotto-Lavino, E., Du, G., and Frohman, M. A. (2006) 3′-End cDNA amplification using classic RACE. *Nat. Protoc.* **1,** 2742–2745 CrossRef Medline
31. Arvaniti, E., Moulos, P., Vakrakou, A., Chatziantoniou, C., Chadjichristos, C., Kavvadas, P., Charonis, A., and Politis, P. K. (2016) Whole-transcriptome analysis of UUO mouse model of renal fibrosis reveals new molecular players in kidney diseases. *Sci. Rep.* **6,** 26235 CrossRef Medline
32. Beynon, R., and Bond, J. S. (2000) *Proteolytic Enzymes*, 2nd Ed., pp. 105–130, Oxford University Press, Oxford, UK

33. Xiao, Y., Pollack, D., Nieves, E., Winchell, A., Callaway, M., and Vigodner, M. (2015) Can your protein be sumoylated? A quick summary and important tips to study SUMO-modified proteins. *Anal. Biochem.* **477,** 95–97 CrossRef Medline
34. Ishizawa, K., Xu, N., Loffing, J., Lifton, R. P., Fujita, T., Uchida, S., and Shibata, S. (2016) Potassium depletion stimulates Na-Cl cotransporter via phosphorylation and inactivation of the ubiquitin ligase Kelch-like 3. *Biochem. Biophys. Res. Commun.* **480,** 745–751 CrossRef Medline
35. Argaiz, E. R., Chavez-Canales, M., Ostrosky-Frid, M., Rodriguez-Gama, A., Vazquez, N., Gonzalez-Rodriguez, X., Garcia-Valdes, J., Hadchouel, J., Ellison, D. H., and Gamba, G. (2018) Kidney-specific WNK1 isoform (KS-WNK1) is a potent activator of WNK4 and NCC. *Am. J. Physiol. Renal Physiol.* CrossRef Medline
36. Correa, L. M., Cho, C., Myles, D. G., and Primakoff, P. (2000) A role for a TIMP-3-sensitive, Zn^{2+}-dependent metalloprotease in mammalian gamete membrane fusion. *Dev. Biol.* **225,** 124–134 CrossRef Medline
37. Koumangoye, R., and Delpire, E. (2017) DNPEP is not the only peptidase that produces SPAK fragments in kidney. *Physiol. Rep.* **5,** e13479 CrossRef Medline
38. Williams, C. R., Mistry, M., Mallick, R., Mistry, A., Ko, B., Gooch, J. L., and Hoover, R. S. (2017) Sodium chloride cotransporter upregulation in settings of zinc deficiency offers new insight into blood pressure dysregulation in chronic diseases. *FASEB J.* **31,** 855.1
39. de Los Heros, P., Kahle, K. T., Rinehart, J., Bobadilla, N. A., Vázquez, N., San Cristobal, P., Mount, D. B., Lifton, R. P., Hebert, S. C., and Gamba, G. (2006) WNK3 bypasses the tonicity requirement for K-Cl cotransporter activation via a phosphatase-dependent pathway. *Proc. Natl. Acad. Sci. U.S.A.* **103,** 1976–1981 CrossRef Medline
40. Frenette-Cotton, R., Marcoux, A.-A., Garneau, A. P., Noel, M., and Isenring, P. (2018) Phosphoregulation of K^+-Cl^- cotransporters during cell swelling: novel insights. *J. Cell Physiol.* CrossRef Medline
41. Yang, C. L., Liu, X., Paliege, A., Zhu, X., Bachmann, S., Dawson, D. C., and Ellison, D. H. (2007) WNK1 and WNK4 modulate CFTR activity. *Biochem. Biophys. Res. Commun.* **353,** 535–540 CrossRef Medline
42. Rafiqi, F. H., Zuber, A. M., Glover, M., Richardson, C., Fleming, S., Jouanouić, S., Jouanouić, S., O'Shaughnessy, K. M., and Alessi, D. R. (2010) Role of the WNK-activated SPAK kinase in regulating blood pressure. *EMBO Mol. Med.* **2,** 63–75 CrossRef Medline
43. Markadieu, N., San-Cristobal, P., Nair, A. V., Verkaart, S., Lenssen, E., Tudpor, K., van Zeeland, F., Loffing, J., Bindels, R. J. M., and Hoenderop, J. G. J. (2012) A primary culture of distal convoluted tubules expressing functional thiazide-sensitive NaCl transport. *Am. J. Physiol. Renal Physiol.* **303,** F886–F892 CrossRef Medline
44. Krishnan, N., Lam, T. T., Fritz, A., Rempinski, D., O'Loughlin, K., Minderman, H., Berezney, R., Marzluff, W. F., and Thapar, R. (2012) The prolyl isomerase Pin1 targets stem-loop binding protein (SLBP) to dissociate the SLBP-histone mRNA complex linking histone mRNA decay with SLBP ubiquitination. *Mol. Cell Biol.* **32,** 4306–4322 CrossRef Medline
45. Li, C., Wen, A., Shen, B., Lu, J., Huang, Y., and Chang, Y. (2011) Fast Cloning: a highly simplified, purification-free, sequence- and ligation-independent PCR cloning method. *BMC Biotechnol.* **11,** 92 CrossRef Medline
46. Lobbestael, E., Zhao, J., Rudenko, I. N., Beylina, A., Gao, F., Wetter, J., Beullens, M., Bollen, M., Cookson, M. R., Baekelandt, V., Nichols, R. J., and Taymans, J.-M. (2013) Identification of protein phosphatase 1 as a regulator of the LRRK2 phosphorylation cycle. *Biochem. J.* **456,** 119–128 CrossRef Medline
47. Villa, F., Goebel, J., Rafiqi, F. H., Deak, M., Thastrup, J., Alessi, D. R., and van Aalten, D. M. F. (2007) Structural insights into the recognition of substrates and activators by the OSR1 kinase. *EMBO Rep.* **8,** 839–845 CrossRef Medline

C-terminally truncated, kidney-specific variants of the WNK4 kinase lack several sites that regulate its activity

Adrián Rafael Murillo-de-Ozores, Alejandro Rodríguez-Gama, Silvana Bazúa-Valenti, Karla Leyva-Ríos, Norma Vázquez, Diana Pacheco-Álvarez, Inti A. De La Rosa-Velázquez, Agnieszka Wengi, Kathryn L. Stone, Junhui Zhang, Johannes Loffing, Richard P. Lifton, Chao-Ling Yang, David H. Ellison, Gerardo Gamba and Maria Castañeda-Bueno

J. Biol. Chem. 2018, 293:12209-12221.
doi: 10.1074/jbc.RA118.003037 originally published online June 19, 2018
